Brain Imaging and Behavior (2019) 13:1689–1698
https://doi.org/10.1007/s11682-018-9973-2

ORIGINAL RESEARCH

Machine learning approach to identify a resting-state functional connectivity pattern serving as an endophenotype of autism spectrum disorder

Bun Yamagata[1] · Takashi Itahashi[2] · Junya Fujino[2] · Haruhisa Ohta[2] · Motoaki Nakamura[2] · Nobumasa Kato[2] · Masaru Mimura[1] · Ryu-ichiro Hashimoto[2,3] · Yuta Aoki[2]

Published online: 2 October 2018

Abstract

Endophenotype refers to a measurable and heritable component between genetics and diagnosis, and the same endophenotype is present in both individuals with a diagnosis and their unaffected siblings. Determination of the neural correlates of an endophenotype and diagnosis is important in autism spectrum disorder (ASD). However, prior studies enrolling individuals with ASD and their unaffected siblings have generally included only one group of typically developing (TD) subjects; they have not accounted for differences between TD siblings. Thus, they could not differentiate the neural correlates for endophenotype from the clinical diagnosis. In this context, we enrolled pairs of siblings with an ASD endophenotype (individuals with ASD and their unaffected siblings) and pairs of siblings without this endophenotype (pairs of TD siblings). Using resting-state functional MRI, we first aimed to identify an endophenotype pattern consisting of multiple functional connections (FCs) then examined the neural correlates of FCs for ASD diagnosis, controlling for differences between TD siblings. Sparse logistic regression successfully classified subjects as to the endophenotype (area under the curve = 0.78, classification accuracy = 75%). Then, a bootstrapping approach controlling for differences between TD siblings revealed that an FC between the right middle temporal gyrus and right anterior cingulate cortex was substantially different between individuals with ASD and their unaffected siblings, suggesting that this FC may be a neural correlate for the diagnosis, while the other FCs represent the endophenotype. The current findings suggest that an ASD endophenotype pattern exists in FCs, and a neural correlate for ASD diagnosis is dissociable from this endophenotype. (250 words).

Keywords Autism spectrum disorder · Endophenotype · Machine learning · Resting state · Unaffected siblings

Introduction

Autism spectrum disorder (ASD) is a developmental disorder characterized by deficits in social interaction (American Psychiatric Association 2013). Consistent with the findings that social interactions depend on the social brain neural system (Adolphs 2009), abnormalities within the social brain have been observed among individuals with ASD (Aoki et al. 2015; Kana et al. 2009; Kleinhans et al. 2016; Murphy et al. 2017; Pelphrey et al. 2011). As individuals with ASD consistently present with atypical functional connections (FCs) (Cherkassky et al. 2006; Di Martino et al. 2014; Uddin et al. 2013), atypical FCs within the social brain are of interest, and they may underlie the impairment in social interactions present in individuals with ASD.

Bun Yamagata and Takashi Itahashi contributed equally to this work.

Electronic supplementary material The online version of this article (https://doi.org/10.1007/s11682-018-9973-2) contains supplementary material, which is available to authorized users.

✉ Yuta Aoki
yuaoki-tky@umin.ac.jp

[1] Department of Neuropsychiatry, Keio University School of Medicine, Tokyo, Japan

[2] Medical Institute of Developmental Disabilities Research, Showa University, 6-11-11 Kitakarasuyama, Tokyo 157-8577, Japan

[3] Department of Language Sciences, Graduate School of Humanities, Tokyo Metropolitan University, Tokyo, Japan

ASD is a highly heritable condition (Colvert et al. 2015); indeed, although the prevalence of ASD is about 1% in the general population (Autism,, and Developmental Disabilities Monitoring Network Surveillance Year Principal, I 2014), the risk of developing ASD increases by up to 20% among biological siblings of individuals with ASD (Ozonoff et al. 2011). Despite such obvious heritability, the concordance for clinical diagnoses among monozygotic twins is only about 60%, indicating that ASD is a consequence of complex genetic contributions (Hallmayer et al. 2011).

The term endophenotype refers to a measurable and heritable component between genes and disease diagnosis (Gottesman and Gould 2003). As ASD is a consequence of complex genetic contributions, characterization of the ASD endophenotype is particularly important, as it may provide an objective intermediate marker and an insight into the pathophysiology of ASD. Resting-state functional magnetic resonance imaging (R-fMRI) has consistently shown abnormalities among individuals with ASD (Di Martino et al. 2014; Glahn et al. 2010), and is a promising modality for differentiating the ASD endophenotype (Khadka et al. 2013).

To identify the ASD endophenotype, prior neuroimaging studies have enrolled individuals with ASD, their unaffected siblings, and typically developing (TD) individuals (Barnea-Goraly et al. 2010; Jou et al. 2016; Moseley et al. 2015). These studies recognized the abnormality shared by individuals with ASD and their unaffected siblings as the ASD endophenotype. However, as these prior studies had not enrolled siblings of TD individuals, they may have underestimated the differences between individuals with ASD and their unaffected siblings. As a result, they did not reveal the neural correlates of a clinical diagnosis of ASD.

To overcome such a potential drawback, we performed this study with two different aims. First, we aimed to classify pairs of siblings in respect to the ASD endophenotype using a multivariate machine learning approach. Second, we examined neural correlates for ASD diagnosis, controlling for the differences between TD siblings. To do this, we obtained R-fMRI data from 60 participants, consisting of 30 people with ASD endophenotype (15 individuals with ASD and 15 of their unaffected siblings) and 30 people without the ASD endophenotype (15 pairs of TDs). As ASD is characterized by the impairment of social interactions, we focused on FCs within the social brain. To increase the homogeneity of the participants, we enrolled only male subjects without intellectual disabilities.

Materials and methods

Participants

We analyzed data from 60 adult males consisting of 30 pairs of biological siblings. Thirty people had the ASD endophenotype. Specifically, 15 pairs of participants were discordant for the diagnosis of ASD: namely, one of the siblings was affected with ASD while the other was unaffected. The other 30 people did not have the endophenotype and consisted of 15 pairs of TD siblings. None of the TD siblings had a family member who had been diagnosed as having ASD. All the participants with ASD were diagnosed by experienced psychiatrists according to the DSM-IV-TR (American Psychiatric, A 2000). The diagnosis was further supported by the Autism Diagnostic Observation Schedule (ADOS) (Lord et al. 2001). In addition, to confirm the absence of a diagnosis of ASD in the unaffected sibling, the parents of the siblings discordant for the diagnosis of ASD were interviewed using the Autism Diagnostic Interview-Revised (ADI-R) (Tsuchiya et al. 2013). We used the Edinburgh Handedness Inventory to evaluate handedness (Oldfield 1971). The intelligence quotient (IQ) of each participant was assessed using either the Wechsler Adult Intelligence Scale-Third Edition or the WAIS-Revised (Wechsler 1997; Wechsler and De Lemos 1981). All the participants completed the Japanese version of the Autism-Spectrum Quotient (AQ) (Wakabayashi et al. 2006). Psychiatric comorbidities were observed in two participants with ASD: one had attention-deficit/hyperactivity disorder, while the other had learning disabilities. Five of the participants were taking medication at the time of scanning: benzodiazepine ($n = 3$), anti-depressants ($n = 3$), and a psychostimulant ($n = 1$). For inclusion in the TD group, we confirmed the absence of an ASD diagnosis among the family members and the absence of an Axis I diagnosis according to the DSM-IV-TR using the Mini-International Neuropsychiatric Interview (Hergueta et al. 1998). The absence of a history of psychotropic medication use was also required. Exclusion criteria for all the participants included known genetic diseases, an estimated full IQ of 80 or below, and a total AQ score of 33 or above. Written informed consent was obtained from all the participants, after they had received a complete explanation of the study. The Ethics Committee of Showa University approved the study protocol. The study was prepared in accordance with the ethical standards of the Declaration of Helsinki.

MRI acquisition

All MRI data were acquired using a 3.0-T MRI scanner (MAGNETON Verio, Siemens Medical Systems, Erlangen, Germany) with a 12-channel head coil. Functional images were acquired for a duration of 10 min 10 s (244 volumes) using an echo-planar imaging sequence (repetition time [TR]: 2500 ms, echo time [TE]: 30 ms, flip angle: 80°, field of view [FOV]: 212 × 212 mm, matrix size: 64 × 64, slice thickness: 3.2 mm with a 0.8-mm gap, 40 axial slices). During the resting-state scans, participants were asked to gaze at a cross-hair displayed at the center of the screen, and were

instructed not to think about specific things and to stay awake. To correct distortion in the functional images, gradient echo field-mapping images were acquired immediately after the resting-state scans (TR: 488 ms, short TE: 4.92 ms, long TE: 7.38 ms, flip angle: 60°, FOV: 212 × 212 mm, matrix size: 64 × 64, slice thickness: 3.2 mm with a 0.8-mm gap, 40 axial slices). To permit normalization of the functional images to standard space coordinates, a T1-weighted image was acquired using an MPRAGE sequence (TR: 2.3 s, TE: 2.98 ms, flip angle: 9°, FOV: 256 × 256 mm, matrix size: 256 × 256, slice thickness: 1 mm, 240 sagittal slices, voxel size: 1 × 1 × 1 mm).

R-fMRI data preprocessing

All the functional images were preprocessed using Statistical Parametric Mapping (SPM12; Wellcome Department of Cognitive Neurology, London, UK) and functions implemented in FMRIB's Software Library (FSL; https://fsl.fmrib.ox.ac.uk/fsl/fslwiki/). Preprocessing was performed as follows: 1) the first four volumes were discarded to allow for T1 equilibration; 2) slice timing correction; 3) head motion correction using mcflirt implemented in FSL (Jenkinson et al. 2002), 4) distortion correction using FUGUE implemented in FSL, 5) co-registration of functional images to the subject's anatomical image, 6) spatial normalization and resampling to a resolution of 2 × 2 × 2 mm, and 7) spatial smoothing (6-mm full-width at half-maximum).

ICA-AROMA was applied (Pruim et al. 2015a; b) to remove the effects of subtle head motions that occurred during the scanning (Power et al. 2012). Following application of the ICA-AROMA, nuisance signals consisting of signals averaged over the white matter, cerebrospinal fluid, and grey matter were regressed out (Parkes et al. 2017; Yahata et al. 2016). A band-pass filter (0.008–0.1 Hz) was then applied to the residual time-series in a voxel-wise manner. For each participant, the mean frame-wise displacement (FD) was calculated from the head motion parameters to quantify the amount of head motion during the scans (Jenkinson et al. 2002). The mean FD of each group is shown in Table 1.

The social brain connectome atlas was used for network construction (Alcala-Lopez et al. 2017). This atlas consists of 36 brain regions associated with social functioning, such as theory of mind, empathy, and facial emotion recognition. For each participant, the mean time-series was extracted from each region of interest (ROI) and the correlation coefficients between all possible pairs of ROIs were calculated, resulting in a 36 × 36 correlation matrix for each participant. Fisher's *r*-to-*z* transformation was then applied to each correlation coefficient. Finally, the lower part of the correlation matrix below the diagonal elements was extracted for each participant, resulting in 630 FCs for each participant.

Statistical analysis

Identification of the endophenotype pattern of FCs

As our aim was to identify a pattern of FCs serving as an endophenotype for a given dataset, we formulated the problem in the following manner. Based on previous findings that individuals with ASD and their unaffected siblings share a pattern of alterations when compared with TDs (Moseley et al. 2015), we recognized that endophenotype was a measurable component satisfying the following conditions:

1. individuals with ASD hold higher values of the weighted linear sum (WLS) of endophenotype-related FCs than TDs (i.e., ASD > TD);
2. unaffected siblings of individuals with ASD also hold higher values than TDs (i.e., unaffected sibling > TD);
3. TD sibling pairs hold similar values (i.e., TD ≅ TD sibling).

According to conditions (1) and (2), our aim could be achieved by solving a classification problem intended to identify FCs capable of discriminating persons with a high value in the WLS of endophenotype-related FCs from persons with a low endophenotype value. Throughout this manuscript, individuals with ASD and their unaffected siblings were regarded as having the ASD endophenotype, while TD and TD siblings were regarded as not having the endophenotype.

To examine whether the FCs serve as an endophenotype, we employed sparse logistic regression (SLR) (Yamashita et al. 2008). SLR can train a logistic regression model while automatically selecting endophenotype-related FCs, without requiring nested cross validation for hyperparameter tuning. Briefly, SLR relies on a hierarchical Bayesian estimation, in which the prior distribution of each element of the parameter vector is represented as a Gaussian distribution. Based on automatic relevance determination, irrelevant features are automatically detected and are not used in the classification because the respective Gaussian prior distributions have a sharp peak at zero. Such an efficient feature elimination method implemented in SLR can mitigate the problems of overfitting caused by a small sample size. Leave-one-pair-out cross-validation (LOPOCV) was performed to evaluate the performance of the classifier (the term 'pair' stands for sibling pairs here). In each fold, all but one pair were used to train the SLR classifier, while the remaining pair was used for evaluation.

A permutation test was performed to further examine the statistical significance of the classification accuracy. At each iteration, a permuted dataset was generated by shuffling the endophenotype label while keeping the pair information. Then, LOPOCV was performed to calculate the classification accuracy for the permuted dataset. This procedure was

Table 1 Characteristics of the participants

	Participants with endophenotype ($n = 30$)				Statistics (a)			Participants without endophenotype (n = 30)				Statistics (d)		
	ASD		Unaffected siblings		df	t	P	TD (b)		TD (c)		df	t	P
	($n = 15$)		(n = 15)					(n = 15)		(n = 15)				
	Mean	SD	Mean	SD				Mean	SD	Mean	SD			
Age (years)	28.3	6.1	28	7.3	14	0.45	0.657	28.4	6.5	25.1	5.3	14	5.62	<0.001
Full IQ	111.8	16	107.4	13.2	14	0.77	0.452	115.9	15.7	114.9	12.1	14	0.24	0.815
Verbal IQ	106.3	31.2	107.1	16.8	14	0.08	0.94	117.1	15.9	116.7	12.5	14	0.18	0.859
Performance IQ	108.1	16.4	105.3	9.8	14	0.62	0.547	109.4	13.6	107.7	7.9	14	0.42	0.678
Handedness	61.8	68.4	99.3	2.9	14	2.11	0.054	89.2	26.4	80.7	51.4	14	0.55	0.594
ADI-R*														
Social interaction	20.7	6.3	0.8	1.4	13	11.56	<0.001	–	–	–	–	–	–	–
Communication (verbal)	12.6	5	0.4	1.1	13	8.83	<0.001	–	–	–	–	–	–	–
RRB	3.9	2	0	0	13	7.02	<0.001	–	–	–	–	–	–	–
ADOS**														
Communication	4.45	1.13	–	–	–	–	–	–	–	–	–	–	–	–
Social interaction	7.91	2.12	–	–	–	–	–	–	–	–	–	–	–	–
Communication + Social interaction	12.36	2.73	–	–	–	–	–	–	–	–	–	–	–	–
RRB	0.18	0.40	–	–	–	–	–	–	–	–	–	–	–	–
AQ														
Total	34.2	6.2	19.4	6.9	12	6.27	<0.001	17.6	5.5	14.9	6	14	1.12	0.28
AS	7.4	1.6	3.9	1.8	12	6.3	<0.001	4	2.1	3.7	1.4	14	0.54	0.596
ATD	5.4	1.9	3.2	1.9	12	2.67	0.02	3.4	2.1	3.9	1.6	14	0.88	0.396
COM	7.6	1.6	3.6	2.6	12	4.16	0.001	3.1	2.5	2.6	2.3	14	0.5	0.625
IMG	6	2	4.1	1.4	12	2.31	0.04	3.7	1.7	2.8	1.7	14	1.26	0.229
SS	7.9	2	4.5	2.7	12	4.26	0.001	3.4	2.7	2	2.1	14	1.38	0.191
SES (e)	5.5	1.1	5.5	1.1	14	0.2	0.843	5.9	1.2	5.7	1.1	13	0.46	0.655
Mean FD	0.17	0.07	0.14	0.05	14	1.51	0.153	0.16	0.07	0.18	0.10	14	0.687	0.503

(a) Statistics show the results of comparisons between adult males with ASD and their unaffected brothers. (b) Older siblings. (c) Younger siblings. (d) Statistics show the results of comparisons between typical older and younger siblings. (e) A higher score indicates a lower socioeconomic status (Okada et al. 2014). Abbreviations: ADOS-2: Autism Diagnostic Observation Schedule Second Edition, ADI-R: Autism Diagnostic Interview-Revised, AQ: autism-spectrum quotient, AS: attention switching/tolerance of change, ASD: autism spectrum disorder, ATD: attention to detail, COM: communication skills, IMG: imagination, IQ: intelligence quotient, RRB: restricted repetitive behaviors, SD: standard deviation, SES: socioeconomic status, SS: social skills, TD: typical development. *The ADI-R score was missing for one person. **ADOS scores are missing for four people

repeated 5000 times to construct a null distribution. Statistical significance was set at $P < 0.05$.

Binomial test

SLR selects a small number of relevant FCs from a given dataset. To confirm that the FCs selected by the classifier were not randomly selected, the statistical significance of the selection counts was examined using a binomial test. The classifier selected a mean of 8.13 ± 0.94 ($\pm$ SD) FCs out of 630 over the 30 validation folds (see Results). Thus, we assumed a binomial distribution, $Bi(n, p)$, where n stands for the number of validation folds (i.e., $n = 30$), and p stands for the probability of being selected from the set of FCs (i.e., $p = 8/630$).

Relationship between endophenotype-related FCs and clinical phenotype

Once the endophenotype-related FCs had been identified by the classifier with binomial tests, we predicted the severity of the clinical symptoms measured by the ADOS. The score for each individual was predicted using LASSO with nine FCs consistently selected in the classifier (Tibshirani 1996). While an optimal regularization parameter for the LASSO was determined by an internal 10-fold CV, the weight parameters were determined through a leave-one-subject-out CV (LOSOCV), in which the scores of all but one participant were linearly regressed using the nine FCs as explanatory variables.

Given the notion that age-related differences might have an impact on the severity of clinical symptoms (Lee et al. 2017), we added age as an additional explanatory variable. The matching of the predicted and actual scores was evaluated using correlation coefficients. We also examined the extent to which the FCs were significantly correlated with the severity of clinical symptoms. Because of the explorative nature of this analysis, we used a liberal statistical threshold of $P < 0.05$.

Bootstrapping

To account for the difference in FC between TD siblings, we adopted a bootstrapping approach with 5000 iterations. At each iteration we resampled the birth order of TD siblings and computed the difference in FCs between older and younger brothers to estimate the distribution of the differences of the FCs. We also calculated the actual difference in FCs between individuals with ASD and their unaffected siblings. Then, we overlaid the actual difference between individuals with ASD and their unaffected siblings onto the estimated distribution of the difference between TD siblings, and computed the percentile rank (Yamagata et al. 2018). We applied these procedures to only the nine FCs that contributed to the endophenotype (see Results). Given that individuals with ASD consistently showed long distance under-connectivity, we recognized a significant finding if the difference between an individual with ASD and their unaffected sibling was in the 95th percentile or above of the TD distribution.

Results

Identification of an endophenotype pattern in the FCs

We discriminated participants with the ASD endophenotype (i.e., individuals with ASD and their unaffected siblings) from TDs using an SLR with LOPOCV. This classifier separated participants with the ASD endophenotype from TDs with 75% accuracy (sensitivity = 76.67% and specificity = 73.33%) and an area under the curve (AUC) of 0.78 (permutation test with 5000 iterations, $p < 0.001$; Fig. 1a, b), suggesting that the FCs selected by this classifier captured the endophenotype-related features.

Post hoc paired *t*-tests were performed to examine whether the conditions (see Methods) were satisfied. As shown in Fig. 1c, paired *t*-tests demonstrated that the WLS of FCs selected in the classifier were not significantly different between individuals with ASD and their unaffected siblings (*t*-value = −0.03, $df = 14$, $p = 0.98$). In contrast, a two-sample *t*-test showed statistically significant differences between people with the ASD endophenotype (i.e., individuals with ASD and their unaffected siblings) and those without the endophenotype (*t*-value = 10.28, $df = 58$, $p < 0.001$). These results indicate that the WLS of FCs selected by the classifier satisfied the set of conditions regarding endophenotype but not the clinical diagnosis. Furthermore, the analysis did not show any significant difference between TD sibling pairs (*t*-value = 1.14, $df = 14$, $p = 0.27$).

To rule out the possibility that nuisance covariates (i.e., head motion and age) had the potential to be important features for the classification, we repeated the same classification analysis with the two nuisance variables added as additional explanatory variables (i.e., 630 FCs + 2 nuisance variables). If the nuisance variables could explain the endophenotype label better than the previously selected FCs, the SLR would automatically select these nuisance variables as inputs for the logistic function. We confirmed that the classification accuracy and the AUC did not change when these nuisance variables were added (accuracy = 75% and AUC = 0.78). Furthermore, in each fold, the SLR never selected the two nuisance variables as inputs for the logistic function (i.e., the weighted parameters for these variables were zero).

Binomial test

We further investigated which FCs were stably selected by the SLR across the LOPOCV. In each fold, the classifier selected a mean of 8.13 ± 0.94 (± SD) FCs across the 30 validation folds, out of a total of 630, and we counted how many times each FC was selected. Under the null hypothesis that eight FCs were randomly selected from 630 FCs, a binomial test was applied to examine the probability of the selection count. We found that nine FCs were selected at a significant frequency ($p < 0.05$, Bonferroni corrected for 630 connections; Fig. 2 and Table 2). The selection count for these nine FCs was 22.78 ± 7.61, while that for the remaining FCs was 0.0627 ± 0.33. This result indicates that the nine FCs were consistently selected across the validation folds.

Relationship between endophenotype-related FCs and clinical phenotype

We predicted the severity of the clinical symptoms measured by the ADOS using the nine FCs identified in the endophenotype classifier. LASSO with LOSOCV was individually applied to determine the weights of the nine FCs so that their weighted linear summation could be used as a predictor for the corresponding severity score. We found that the communication domain of the ADOS was well predicted from the nine FCs, with a statistically significant correlation ($r = 0.68$, $p = 0.021$; Fig. 3a). Furthermore, we found that two of the nine FCs were significantly correlated with the severity of impaired communication measured by ADOS: one was the FC between

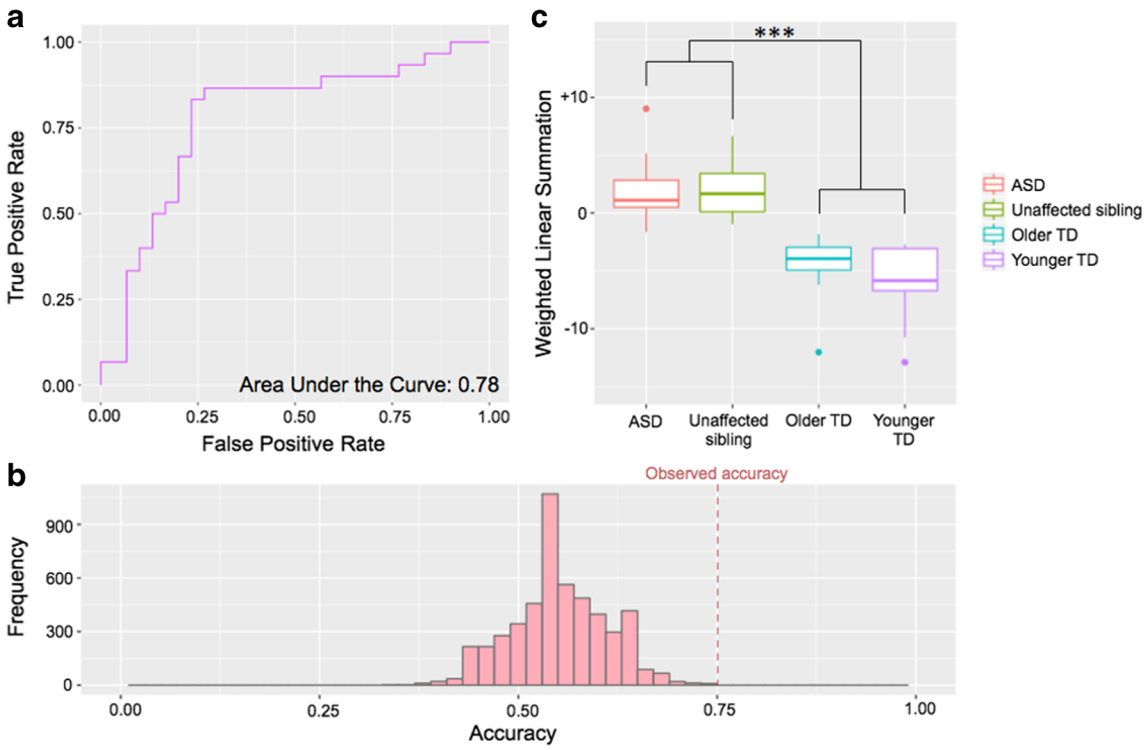

Fig. 1 Classification results and post hoc tests. **a** Receiver operating characteristic curve. A sparse logistic regression with leave-one-pair-out cross validation exhibited an area under the curve of 0.78. **b** Null distribution of classification accuracy derived from a permutation test with 5000 iterations. The permutation test demonstrated that the observed classification accuracy (75%) was significantly higher than that obtained by the permuted classifier ($p < 0.001$). **c** Post hoc paired *t*-tests demonstrated that there were no statistically significant differences in the weighted linear summation of selected FCs between individuals with autism spectrum disorder (ASD) and their unaffected siblings (*t*-value = −0.03, $df = 14$, $p = 0.98$), as well as between TD pairs (*t*-value = 1.14, $df = 14$, $p = 0.27$). However, those with the endophenotype exhibited significantly higher values than those without the endophenotype (*t*-value = 10.28, $df = 58$, $p < 0.001$). ***: $P < 0.001$

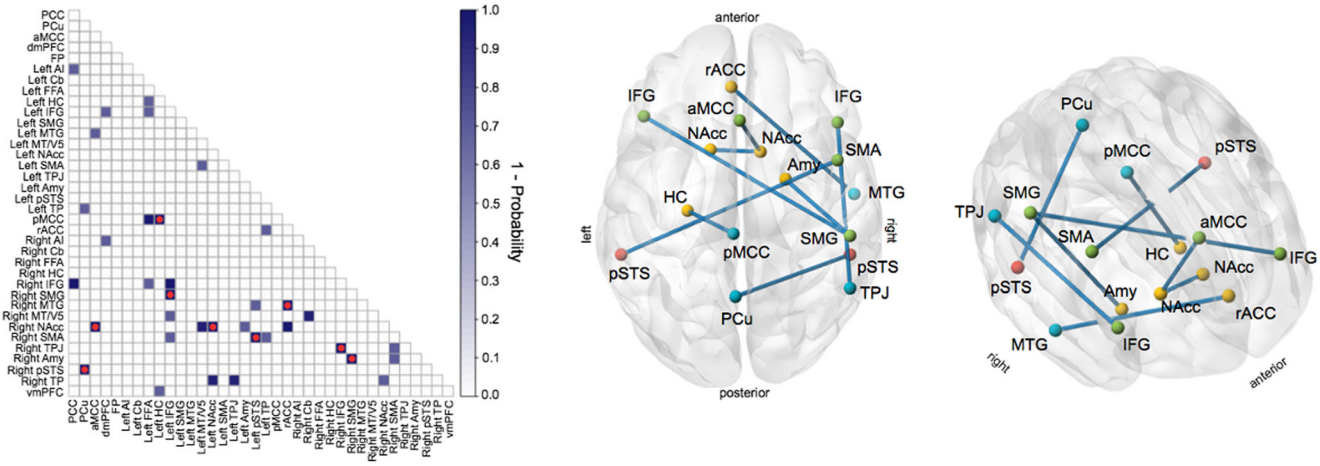

Fig. 2 Stable functional connections (FCs) identified and selected for the classification. The left panel shows the results of binomial tests. The red circle indicates the statistical significance of the selected count after multiple comparison correction. The right panel displays the distribution of nine FCs exhibiting statistical significance after multiple comparison corrections. The colors of the nodes represent the sub-systems within the social brain atlas defined in Alcala-Lopez et al. (2017). Red: visual-sensory system, Yellow: limbic system, Green: intermediate-level system, Cyan: higher-level system. **Abbreviations:** ACC: anterior cingulate cortex, AI: anterior insula, aMCC: anterior middle cingulate cortex, Amy: amygdala, Cb: cerebellum, dmPFC: dorsomedial prefrontal cortex, FFA: fusiform face area, FP: frontal pole, HC: hippocampal cortex, IFG: inferior frontal gyrus, MT/V5: middle temporal V5 area, MTG: middle temporal gyrus, NAcc: nucleus accumbens, PCC: posterior cingulate cortex, PCu: precuneus, pSTS: posterior superior temporal sulcus, SMA: supplementary motor area, SMG: supramarginal gyrus, TPJ: temporo-parietal junction, vmPFC: ventromedial prefrontal cortex

Table 2 Functional connections (FCs) consistently selected for classification

ID	Terminal region 1			Terminal region 2			Mean weight
	Name	Hemi.	Sub-system	Label	Hemi.	Sub-system	
1	SMA	R	Intermediate	pSTS	L	Visual-sensory	5.75
2	TPJ	R	Higher	IFG	R	Intermediate	2.42
3	NAcc	R	Limbic	NAcc	L	Limbic	−0.81
4	pMCC	L	Intermediate	HC	L	Limbic	−3.02
5	pSTS	R	Visual-sensory	Pcu	M	Higher	−5.71
6	NAcc	R	Limbic	aMCC	M	Intermediate	−6.49
7	Amy	R	Limbic	SMG	R	Intermediate	−6.69
8	SMG	R	Intermediate	IFG	L	Intermediate	−6.84
9	MTG	R	Higher	rACC	M	Limbic	−7.75

Brain regions and sub-systems were based on Alcala-Lopez et al. (2017)

aMCC anterior middle cingulate cortex; *Amy* amygdala; *HC* hippocampal cortex; *Hemi* hemisphere; *IFG* inferior frontal gyrus; *L* left; *M* middle; *MTG* middle temporal gyrus; *NAcc* nucleus accumbens; *PCu* precuneus; *pMCC* posterior medial cingulate cortex; *pSTS* posterior superior temporal sulcus; *R* right; *rACC* rostral anterior cingulate cortex; *SMA* supplementary motor area; *SMG* supramarginal gyrus; *TPJ* temporo-parietal junction

the right temporo-parietal junction and right inferior frontal gyrus ($r = 0.81$, $p = 0.0026$; Fig. 3b), and the other was the FC between the right nucleus accumbens and the anterior middle cingulate cortex ($r = -0.60$, $p = 0.049$; Fig. 3c).

Bootstrapping

A bootstrapping approach with 5000 iterations revealed that the difference in the FC between the right middle temporal gyrus (MTG) and right anterior cingulate cortex (ACC) between individuals with ASD and their unaffected siblings was in the 97th percentile of the distribution representing the differences in the same FC between TD siblings (Table 3).

Discussion

Our novel framework was motivated by the fact that prior studies on ASD endophenotype did not account for the differences between TD siblings. Thus, we enrolled not only siblings with the ASD endophenotype, but also pairs of TD siblings. We then applied a machine learning approach to examine the ASD endophenotype, with the subsequent binomial tests identifying nine FCs that together served as the potential endophenotype. Taking advantage of the strength of our study participant selection, we conducted a bootstrapping approach to examine whether the differences between individuals with ASD and their unaffected siblings were accounted for by the

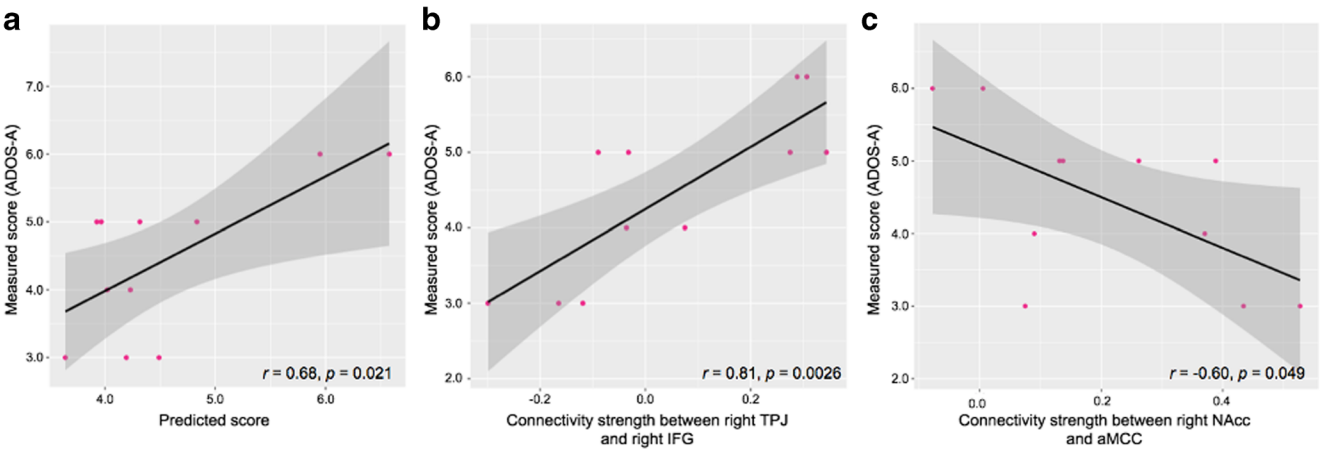

Fig. 3 Associations between the severity of clinical symptoms and functional connections (FCs) selected by the classifier. a Prediction of the severity of communication impairment measured by the Autism Diagnostic Observation Schedule (ADOS) using the least absolute shrinkage and selection operator with leave-one-subject-out cross-validation. The correlation coefficient between the predicted and measured scores exhibited a significant positive correlation ($r = 0.68$, $p = 0.021$). **b** The connectivity strength between the right temporo-parietal junction and right inferior frontal gyrus was significantly correlated with the severity of impaired communication as measured by the ADOS-A ($r = 0.81$, $p = 0.0026$). **c** The connection strength between the right nucleus accumbens and anterior middle cingulate cortex was significantly correlated with the severity of communication impairment measured by the ADOS-A ($r = -0.60$, $p = 0.049$)

Table 3 Results of the bootstrapping

FCs	Percentile
rpSTS_PCu	74
rNAcc_aMCC	34
lpMCC_lHC	54
rSMG_lIFG	38
rNAcc_lNAcc	44
rSMA_lpSTS	82
rMTG_rACC	97
rTPJ_rIFG	29
rAmy_rSMG	75

aMCC anterior middle cingulate cortex; *Amy* amygdala; *HC* hippocampal cortex; *Hemi* hemisphere; *IFG* inferior frontal gyrus; *L* left; *M* middle; *MTG* middle temporal gyrus; *NAcc* nucleus accumbens; *PCu* precuneus; *pMCC* posterior middle cingulate cortex; *pSTS* posterior superior temporal sulcus; *R* right; *rACC* rostral anterior cingulate cortex; *SMA* supplementary motor area; *SMG* supramarginal gyrus; *TPJ* temporo-parietal junction

differences between TD siblings, and revealed that one of the FCs identified as belonging to the potential ASD endophenotype was related to the clinical diagnosis. Again, with a novel framework, we differentiated FCs related to the ASD endophenotype and to the ASD diagnosis.

We utilized the SLR to classify participants according to ASD endophenotype. Most prior neuroimaging studies identified abnormalities shared by individuals with ASD and their unaffected siblings, or abnormalities in the siblings that were intermediate between ASD and TD as an endophenotype (Barnea-Goraly et al. 2010; Jou et al. 2016; Moseley et al. 2015). In these studies, each variable (i.e., connectivity index) was separately examined to determine whether it belonged to the endophenotype. In contrast, we applied a multivariate and data-driven approach to classify individuals with or without the ASD endophenotype using all the available variables (i.e., 630 FC correlations within the social brain). This approach inherently assumes that the endophenotype emerges as a pattern of altered FCs and allows all the variables to contribute to the endophenotype to different extents. In the case of ASD, the genetic abnormalities vary across individuals (Geschwind and Levitt 2007; Miles 2011), and multiple FCs are altered (Di Martino et al. 2014; Uddin et al. 2013). Thus, the genetic influence does not show an identical pattern of FCs across people (Ameis and Szatmari 2012; Meyer-Lindenberg and Weinberger 2006; Zhan et al. 2014), and the endophenotype should emerge as multiple FCs with different extents. The consistency of our methodology with the definition of the endophenotype might explain the good performance in the classification.

The current study identified an ASD endophenotype among the FCs within the social brain. As not all individuals with the endophenotype develop a clinical diagnosis of ASD (Ozonoff et al. 2011), the neural correlates for the endophenotype and the diagnosis may differ. Given that there was no significant difference in the WLS of the selected FCs between individuals with ASD and their unaffected siblings, the selected FCs may represent the ASD endophenotype. However, with the bootstrapping approach, we identified one of the nine FCs as being substantially different between individuals with ASD and unaffected siblings. These results suggest that the FC between the right MTG and right ACC may be related to development of a clinical diagnosis of ASD among people at risk, while other FCs are related to the endophenotype. Although the current results are far from a clinical application, they may provide a potential future direction for research into the development of ASD.

Using LASSO, the selected FCs successfully predicted the severity of communication deficits among individuals with ASD. The relationship between FCs and ASD-related symptoms corroborates the assumption that the selected FCs are associated with the pathophysiology of ASD. As we lacked any ADOS scores from the unaffected siblings of individuals with ASD, this relationship was observed only among the individuals with ASD. However, even if the ADOS scores were available from the unaffected siblings, the scores might not be a good reflection of the distribution of behavior, since the ADOS aims to measure clinical symptoms, not subclinical ones observed among people with the ASD endophenotype (Toth et al. 2007). Future studies enrolling unaffected siblings should obtain both MRI data and psychological evaluations that reflect the differences in ASD traits among subclinical individuals.

Several limitations to this study should be considered. First, although we successfully added the condition that the FCs should not differ between TD siblings (see Method), which was not possible in prior studies with only one TD group, the current study had a small sample size because of practical difficulties in recruitment. Thus, because of the lack of statistical power, we could not address brain regions outside of the social brain. However, brain regions outside the social brain are also likely to be involved in the endophenotype of ASD. In addition, although the sparseness of FC selection by the SLR mitigates over-fitting to the current sample, the current sample size was relatively small in comparison with the number of FCs. However, simulations demonstrated that despite the limited sample size, SLR could achieve a high classification performance (see Supplementary Materials), providing support for the applicability of SLR to our dataset. Further extensive simulations might provide an indication of the minimum number of subjects appropriate for a supervised machine learning algorithm. In addition, given that both individuals with ASD and their unaffected siblings hold the ASD endophenotype, the between-group contrast between the group containing individuals with ASD and their unaffected siblings and the TD siblings group should encompass the ASD endophenotype.

However, combining individuals with ASD with their unaffected siblings increased the heterogeneity of the participants because of the difference in the clinical diagnoses. Indeed, confirmatory analysis revealed that two out of nine FCs might be relevant to the clinical diagnosis, rather than the ASD endophenotype (see Supplementary Materials). A future study with a sample size large enough to avoid over-fitting and combining individuals with ASD and their unaffected siblings is needed. Second, although the machine learning approach successfully classified individuals with or without the ASD endophenotype, the endophenotype may not be categorical, as is the case with ASD diagnosis (Aoki et al. 2017). Research using a large sample is encouraged to stratify individuals with an ASD endophenotype. Third, to increase the homogeneity of participants, we recruited only adult males in the current study. Given that the ASD brain shows an atypical developmental trajectory (Aoki et al. 2012), the current finding may not be generalizable to other age ranges. In addition, atypical sex differences have been observed among individuals with ASD (Lai et al. 2017). Thus, further studies that include only female ASD participants are required.

Conclusion

Using the machine learning approach, we demonstrated that the ASD endophenotype emerges as a pattern of FCs within the social brain. One of the selected FCs showed a substantial difference between individuals with ASD and their unaffected siblings when controls were made for the differences between TD siblings. These results suggest that this particular FC is related to the development of the clinical diagnosis of ASD, while the others are associated with the endophenotype.

Acknowledgements This study is the result of "Development of BMI Technologies for Clinical Application" carried out under the Strategic Research Program for Brain Sciences by the Japan Agency for Medical Research and Development (AMED). This work is partly supported by a grant from The Japan Foundation for Pediatric Research (to YA).

Funding This study is the result of "Development of BMI Technologies for Clinical Application" carried out under the Strategic Research Program for Brain Sciences by the Japan Agency for Medical Research and Development (AMED). This work is partly supported by a grant from The Japan Foundation for Pediatric Research (to YA).

Compliance with ethical standards

Conflict of interest All authors report no conflict of interest.

Ethical approval The study was prepared in accordance with the ethical standards of the Declaration of Helsinki.

Informed consent Written informed consent was obtained from all the participants, after they had received a complete explanation of the study.

References

Adolphs, R. (2009). The social brain: Neural basis of social knowledge. *Annual Review of Psychology, 60*, 693–716.

Alcala-Lopez, D., Smallwood, J., Jefferies, E., Van Overwalle, F., Vogeley, K., Mars, R. B., et al. (2017). Computing the social brain connectome across systems and states. *Cereb Cortex* (1460-2199 (electronic)), 1-26.

Ameis, S. H., & Szatmari, P. (2012). Imaging-genetics in autism spectrum disorder: Advances, translational impact, and future directions. *Frontiers in Psychiatry, 3*, 46.

American Psychiatric, A. (2000). *Diagnostic and statistical manual, 4th edn, text revision (DSM-IV-TR)*. Washington: American Psychiatric Association.

American Psychiatric Association. (2013). *Diagnostic and statistical manual of mental disorders (DSM-5®)*. Arlington, VA: American Psychiatric Association.

Aoki, Y., Kasai, K., & Yamasue, H. (2012). Age-related change in brain metabolite abnormalities in autism: A meta-analysis of proton magnetic resonance spectroscopy studies. *Translational Psychiatry, 2*, e69.

Aoki, Y., Cortese, S., & Tansella, M. (2015). Neural bases of atypical emotional face processing in autism: A meta-analysis of fMRI studies. *The World Journal of Biological Psychiatry, 16*(5), 291–300.

Aoki, Y., Yoncheva, Y. N., Chen, B., Nath, T., Sharp, D., Lazar, M., Velasco, P., Milham, M. P., & di Martino, A. (2017). Association of white matter structure with autism spectrum disorder and attention-deficit/hyperactivity disorder. *JAMA Psychiatry, 74*(11), 1120–1128.

Autism, & Developmental Disabilities Monitoring Network Surveillance Year Principal, I. (2014). Prevalence of autism spectrum disorder among children aged 8 years—Autism and developmental disabilities monitoring network, 11 sites, United States, 2010. *Morbidity and Mortality Weekly Report. Surveillance Summaries, 63*(2), 1–21.

Barnea-Goraly, N., Lotspeich, L. J., & Reiss, A. L. (2010). Similar white matter aberrations in children with autism and their unaffected siblings: A diffusion tensor imaging study using tract-based spatial statistics. *Archives of General Psychiatry, 67*(10), 1052–1060.

Cherkassky, V. L., Kana, R. K., Keller, T. A., & Just, M. A. (2006). Functional connectivity in a baseline resting-state network in autism. *Neuroreport, 17*(16), 1687–1690.

Colvert, E., Tick, B., McEwen, F., Stewart, C., Curran, S. R., Woodhouse, E., Gillan, N., Hallett, V., Lietz, S., Garnett, T., Ronald, A., Plomin, R., Rijsdijk, F., Happé, F., & Bolton, P. (2015). Heritability of autism spectrum disorder in a UK population-based twin sample. *JAMA Psychiatry, 72*(5), 415–423.

Di Martino, A., Yan, C.-G., Li, Q., Denio, E., Castellanos, F. X., Alaerts, K., et al. (2014). The autism brain imaging data exchange: Towards a large-scale evaluation of the intrinsic brain architecture in autism. *Molecular Psychiatry, 19*(6), 659–667.

Geschwind, D. H., & Levitt, P. (2007). Autism spectrum disorders: Developmental disconnection syndromes. *Current Opinion in Neurobiology, 17*(1), 103–111.

Glahn, D. C., Winkler, A. M., Kochunov, P., Almasy, L., Duggirala, R., Carless, M. A., Curran, J. C., Olvera, R. L., Laird, A. R., Smith, S. M., Beckmann, C. F., Fox, P. T., & Blangero, J. (2010). Genetic control over the resting brain. *Proceedings of the National Academy of Sciences of the United States of America, 107*(3), 1223–1228.

Gottesman, I. I., & Gould, T. D. (2003). The endophenotype concept in psychiatry: Etymology and strategic intentions. *American Journal of Psychiatry, 160*(4), 636–645.

Hallmayer, J., Cleveland, S., Torres, A., Phillips, J., Cohen, B., Torigoe, T., Miller, J., Fedele, A., Collins, J., Smith, K., Lotspeich, L., Croen, L. A., Ozonoff, S., Lajonchere, C., Grether, J. K., & Risch, N. (2011). Genetic heritability and shared environmental factors among twin pairs with autism. *Archives of General Psychiatry, 68*(11), 1095–1102.

Hergueta, T., Baker, R., & Dunbar, G. C. (1998). The MINI-international neuropsychiatric interview (MINI): The development and validation of a structured diagnostic psychiatric interview for DSM-IVand ICD-10. *Journal of Clinical Psychiatry, 59*(Suppl 20), 2233.

Jenkinson, M., Bannister, P., Brady, M., & Smith, S. (2002). Improved optimization for the robust and accurate linear registration and motion correction of brain images. *Neuroimage, 17*(2), 825–841.

Jou, R. J., Reed, H. E., Kaiser, M. D., Voos, A. C., Volkmar, F. R., & Pelphrey, K. A. (2016). White matter abnormalities in autism and unaffected siblings. *Journal of Neuropsychiatry & Clinical Neurosciences, 28*(1), 49–55.

Kana, R. K., Keller, T. A., Cherkassky, V. L., Minshew, N. J., & Just, M. A. (2009). Atypical frontal-posterior synchronization of theory of mind regions in autism during mental state attribution. *Social Neuroscience, 4*(2), 135–152.

Khadka, S., Meda, S. A., Stevens, M. C., Glahn, D. C., Calhoun, V. D., Sweeney, J. A., Tamminga, C. A., Keshavan, M. S., O'Neil, K., Schretlen, D., & Pearlson, G. D. (2013). Is aberrant functional connectivity a psychosis endophenotype? A resting state functional magnetic resonance imaging study. *Biological Psychiatry, 74*(6), 458–466.

Kleinhans, N. M., Richards, T., Greenson, J., Dawson, G., & Aylward, E. (2016). Altered dynamics of the fMRI response to faces in individuals with autism. *Journal of Autism and Developmental Disorders, 46*(1), 232–241.

Lai, M. C., Lerch, J. P., Floris, D. L., Ruigrok, A. N. V., Pohl, A., Lombardo, M. V., & Baron-Cohen, S. (2017). Imaging sex/gender and autism in the brain: Etiological implications. *Journal of Neuroscience Research, 95*(1–2), 380–397.

Lee, Y., Park, B. Y., James, O., Kim, S. G., & Park, H. (2017). Autism spectrum disorder related functional connectivity changes in the language network in children, adolescents and adults. Frontiers in Human Neuroscience, 11(1662–5161 (Print)), 418.

Lord, C., Rutter, M., DiLavore, P. C., Risi, S., Gotham, K., & Bishop, S. L. (2001). *Autism diagnostic observation schedule (ADOS): Manual*: WPS.

Meyer-Lindenberg, A., & Weinberger, D. R. (2006). Intermediate phenotypes and genetic mechanisms of psychiatric disorders. *Nature Reviews Neuroscience, 7*(10), 818–827.

Miles, J. H. (2011). Autism spectrum disorders—A genetics review. *Genetics in Medicine, 13*(4), 278–294.

Moseley, R. L., Ypma, R. J., Holt, R. J., Floris, D., Chura, L. R., Spencer, M. D., et al. (2015). Whole-brain functional hypoconnectivity as an endophenotype of autism in adolescents. *Neuroimage Clinical, 9*, 140–152.

Murphy, C. M., Christakou, A., Giampietro, V., Brammer, M., Daly, E. M., Ecker, C., Johnston, P., Spain, D., Robertson, D. M., MRC AIMS Consortium, Murphy, D. G., & Rubia, K. (2017). Abnormal functional activation and maturation of ventromedial prefrontal cortex and cerebellum during temporal discounting in autism spectrum disorder. *Human Brain Mapping, 38*(11), 5343–5355.

Okada, N., Kasai, K., Takahashi, T., Suzuki, M., Hashimoto, R., & Kawakami, N. (2014). Brief rating scale of socioeconomic status for biological psychiatry research among Japanese people: A scaling based on an educational history. *Japanese Journal of Biological Psychiatry, 25*, 115–117.

Oldfield, R. C. (1971). The assessment and analysis of handedness: The Edinburgh inventory. *Neuropsychologia, 9*(1), 97–113.

Ozonoff, S., Young, G. S., Carter, A., Messinger, D., Yirmiya, N., Zwaigenbaum, L., Bryson, S., Carver, L. J., Constantino, J. N., Dobkins, K., Hutman, T., Iverson, J. M., Landa, R., Rogers, S. J., Sigman, M., & Stone, W. L. (2011). Recurrence risk for autism spectrum disorders: A baby siblings research consortium study. *Pediatrics, 128*(3), e488–e495.

Parkes, L., Fulcher, B., Yu Cel, M., & Fornitod, A. (2017). An evaluation of the efficacy, reliability, and sensitivity of motion correction strategies for resting-state functional MRI. NeuroImage.

Pelphrey, K. A., Shultz, S., Hudac, C. M., & Vander Wyk, B. C. (2011). Research review: Constraining heterogeneity: The social brain and its development in autism spectrum disorder. *Journal of Child Psychology and Psychiatry, 52*(6), 631–644.

Power, J. D., Barnes, K. A., Snyder, A. Z., Schlaggar, B. L., & Petersen, S. E. (2012). Spurious but systematic correlations in functional connectivity MRI networks arise from subject motion. *Neuroimage, 59*(3), 2142–2154.

Pruim, R. H., Mennes, M., Buitelaar, J. K., & Beckmann, C. F. (2015a). Evaluation of ICA-AROMA and alternative strategies for motion artifact removal in resting state fMRI. *Neuroimage, 112*, 278–287.

Pruim, R. H., Mennes, M., van Rooij, D., Llera, A., Buitelaar, J. K., & Beckmann, C. F. (2015b). ICA-AROMA: A robust ICA-based strategy for removing motion artifacts from fMRI data. *Neuroimage, 112*, 267–277.

Tibshirani, R. (1996). Regression shrinkage and selection via the lasso. *Journal of the Royal Statistical Society: Series B: Methodological*, 267–288.

Toth, K., Dawson, G., Meltzoff, A. N., Greenson, J., & Fein, D. (2007). Early social, imitation, play, and language abilities of young nonautistic siblings of children with autism. *Journal of Autism and Developmental Disorders, 37*(1), 145–157.

Tsuchiya, K. J., Matsumoto, K., Yagi, A., Inada, N., Kuroda, M., Inokuchi, E., Koyama, T., Kamio, Y., Tsujii, M., Sakai, S., Mohri, I., Taniike, M., Iwanaga, R., Ogasahara, K., Miyachi, T., Nakajima, S., Tani, I., Ohnishi, M., Inoue, M., Nomura, K., Hagiwara, T., Uchiyama, T., Ichikawa, H., Kobayashi, S., Miyamoto, K., Nakamura, K., Suzuki, K., Mori, N., & Takei, N. (2013). Reliability and validity of autism diagnostic interview-revised, Japanese version. *Journal of Autism and Developmental Disorders, 43*(3), 643–662.

Uddin, L. Q., Supekar, K., & Menon, V. (2013). Reconceptualizing functional brain connectivity in autism from a developmental perspective. *Frontiers in Human Neuroscience, 7*, 458.

Wakabayashi, A., Baron-Cohen, S., Wheelwright, S., & Tojo, Y. (2006). The autism-Spectrum quotient (AQ) in Japan: A cross-cultural comparison. *Journal of Autism and Developmental Disorders, 36*(2), 263–270.

Wechsler, D. (1997). *WAIS-III: Wechsler adult intelligence scale*: Psychological corporation.

Wechsler, D., & De Lemos, M. M. (1981). *Wechsler adult intelligence scale-revised*: Harcourt brace Jovanovich.

Yahata, N., Morimoto, J., Hashimoto, R., Lisi, G., Shibata, K., Kawakubo, Y., Kuwabara H., Kuroda M., Yamada T., Megumi F., Imamizu H., Náñez Sr J. E., Takahashi H., Okamoto Y., Kasai K., Kato N., Sasaki Y., Watanabe T., Kawato M. (2016). A small number of abnormal brain connections predicts adult autism spectrum disorder. Nature Communications, 7.

Yamagata, B., Itahashi, T., Nakamura, M., Mimura, M., Hashimoto, R. I., Kato, N., Mimura, M., Hashimoto, R. I., Kato, N., & Aoki, Y. (2018). White matter endophenotypes and correlates for the clinical diagnosis of autism spectrum disorder. *Social Cognitive and Affective Neuroscience, 13*, *765–773*.

Yamashita, O., Sato, M. A., Yoshioka, T., Tong, F., & Kamitani, Y. (2008). Sparse estimation automatically selects voxels relevant for the decoding of fMRI activity patterns. *Neuroimage, 42*(4), 1414–1429.

Zhan, Y., Paolicelli, R. C., Sforazzini, F., Weinhard, L., Bolasco, G., Pagani, F., Vyssotski, A. L., Bifone, A., Gozzi, A., Ragozzino, D., & Gross, C. T. (2014). Deficient neuron-microglia signaling results in impaired functional brain connectivity and social behavior. *Nature Neuroscience, 17*(3), 400–406.